



# Quantum impurity approach to a coupled qubit problem

Sebastien Camalet, Josef Schrieffer, Pascal Degiovanni, François Delduc

## ► To cite this version:

Sebastien Camalet, Josef Schrieffer, Pascal Degiovanni, François Delduc. Quantum impurity approach to a coupled qubit problem. EPL - Europhysics Letters, 2004, 68, pp.37. 10.1209/epl/i2004-12019-1 . hal-00001621v2

**HAL Id: hal-00001621**

**<https://hal.science/hal-00001621v2>**

Submitted on 1 Oct 2004

**HAL** is a multi-disciplinary open access archive for the deposit and dissemination of scientific research documents, whether they are published or not. The documents may come from teaching and research institutions in France or abroad, or from public or private research centers.

L'archive ouverte pluridisciplinaire **HAL**, est destinée au dépôt et à la diffusion de documents scientifiques de niveau recherche, publiés ou non, émanant des établissements d'enseignement et de recherche français ou étrangers, des laboratoires publics ou privés.

## Quantum impurity approach to a coupled qubit problem

S. CAMALET<sup>1</sup>, J. SCHRIEFL<sup>1,2</sup>, P. DEGIOVANNI<sup>1</sup> and F. DELDUC<sup>1</sup>

<sup>1</sup> *CNRS-Laboratoire de Physique, Ecole Normale Supérieure de Lyon - 46 allée d'Italie, 69007 Lyon, France*

<sup>2</sup> *Institut für Theoretische Festkörperphysik - Universität Karlsruhe, 76128 Karlsruhe, Germany*

PACS. 32.80.-t – Photon interactions with atoms.

PACS. 71.10.Pm – Fermions in reduced dimensions.

PACS. 72.10.Fk – Scattering by point defects, dislocations, surfaces, and other.

**Abstract.** – We consider a system of two qubits at the ends of a finite length 1D cavity. This problem is mapped onto the double-Kondo model which is also shown to describe the low energy physics of a finite length quantum wire with resonant levels at its ends. At the Toulouse point the ground state energy and the average populations and correlations of the qubits or resonant levels at zero temperature are computed. These results show that the effective interactions between the qubits or resonant levels can be used to probe their associated Kondo length scale.

Cavity quantum electrodynamics (cQED) concerns the study of atoms coupled to discrete quantized electromagnetic modes in a high- $Q$  cavity. Recent experiments performed with Rydberg atoms in a microwave cavity have shown how cQED can be used to create and manipulate entanglement between atoms and the quantized electromagnetic field (see [1] for a review). Experiments performed on a variety of Josephson devices have demonstrated their potentialities as artificial two-level systems suitable for quantum state engineering (see [2] for a review). These considerations motivated a recent proposal [3] for a cQED-type quantum computing architecture based on Cooper pair boxes embedded in a super-conducting transmission line.

All these cQED schemes consider the coupling of a single quantum electromagnetic mode to the qubits and the theoretical analysis is performed using the Jaynes-Cummings Hamiltonian which relies on the rotating wave approximation. However, in a sufficiently large cavity a large number of modes exist. Whereas in the weak coupling regime the single-mode approach and the rotating wave approximation are expected to give correct results, this is not the case when the qubits are strongly coupled to the transmission line. For instance, Leclair *et al.* showed [4,5] that the exact spectrum of a single qubit coupled to an infinite transmission line is considerably richer than the spectrum of the Jaynes-Cummings Hamiltonian. In the same model the average population and fluctuations of the qubit at zero temperature have also been studied [6]. But so far, very little is known on the correlations between several qubits strongly coupled to such an environment. In this regime, neither the Jaynes-Cummings Hamiltonian nor perturbation theory in the qubit/cavity coupling are expected to work. The purpose of

this letter is to study these correlations in the strong coupling regime using techniques and concepts developed in the context of quantum impurity problems.

In this letter, we consider the coupling of two qubits through a transmission line of length  $L$  (see fig. 1). Using a mapping onto the double-Kondo model we study the correlations between the two qubits induced by their interaction via the transmission line. At the Toulouse point of the double-Kondo model we obtain an explicit description of the ground state and low energy excitations of the system. The inter-qubit correlations at  $T = 0$  K are computed exactly and shown to depend on intrinsic length scales associated with each qubit (Kondo lengths). Depending on the ratio of these Kondo lengths to  $L$  the system flows from a Kondo regime where each qubit renormalizes to a conformally invariant boundary condition and is not influenced by the other to a correlated regime where the degrees of freedom of the qubits get dressed and coupled by the transmission line. This crossover occurs when the Kondo lengths associated with each qubits are comparable to the size  $L$  of the system. Kondo cloud physics in a finite system with a single quantum impurity has recently received attention [7]. We point out that any system described by the double-Kondo model provides a way to probe the interplay between Kondo cloud physics and interactions in a finite size system with two quantum impurities.

Originally introduced in string theory within the context of tachyon instabilities [8] the double-Kondo model not only describes the two-qubit problem but may also be relevant in mesoscopic physics. We show that it describes the low energy behavior of a finite length 1D quantum wire coupled by tunnel junctions to two resonant levels (see fig. 2). The quantities of interest are the average occupation numbers of each resonant level and their correlations. The device of fig. 2 may be realized using conventional lithography techniques. We think that it could provide a complementary route to explore the physics of coupled quantum impurities underlying the system of fig. 1.

The quantum circuit of fig. 1 consists of two Josephson charge qubits built from Cooper pair boxes in the charge regime [2] capacitively coupled to a quantum transmission line. For convenience, each qubit is labelled by its position along the transmission line:  $j = -L$  or  $0$ . In the continuum limit the quantum transmission line is described in terms of a free bosonic field  $\Phi(x)$  and its conjugated field  $\Pi(x)$  ( $-L \leq x \leq 0$ ) related to the charge and current densities along the line:

$$i(x, t) = -ev \sqrt{\frac{\hbar/e^2}{\mathcal{R}}} (\partial_x \Phi)(x, t) \quad \text{and} \quad \rho(x, t) = \frac{e}{\hbar} \sqrt{\frac{\hbar/e^2}{\mathcal{R}}} \Pi(x, t) \quad (1)$$

where  $v = 1/\sqrt{lc}$  is the wave velocity along the transmission line and  $\mathcal{R} = \sqrt{l/c}$  is the resistance of the semi-infinite line both expressed in terms of the line's capacitance  $c$  and inductance  $l$  per unit of length. The low-energy effective Hamiltonian of the system depicted on fig. 1 is then:

$$H = -\frac{1}{2} \sum_{j=-L,0} (E_j^J \sigma_j^x + \tilde{B}_j^z \sigma_j^z) + \frac{\hbar v}{2} \int_{-L}^0 (\hbar^{-2} \Pi^2 + (\partial_x \Phi)^2) dx + \frac{v}{2} \sum_{j=-L,0} \beta_j \Pi(j) \cdot (\sigma_j^z + 2n_j^G - 1) \quad (2)$$

where the first term represents the bare qubit Hamiltonian [2]. The effective magnetic field  $\tilde{B}_j^z = 2e^2(1 - 2n_j^G)/(C_j^J + C_j^G)$  depends on the externally controlled gate voltage  $V_j^G$  ( $n_j^G = C_j^G V_j^G / 2e$ ). Here  $C_j^J$  and  $C_j^G$  respectively denote the Josephson junction and gate capacitances of qubit  $j$ . The Josephson energy  $E_j^J$  can be controlled by applying an external flux through the loop of the SQUID device. The second term in (2) is the free transmission line Hamiltonian. The third one couples the qubits to the transmission line with dimensionless

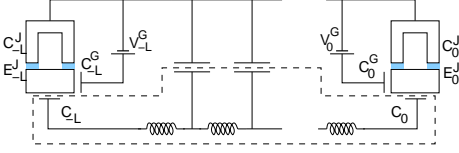


Fig. 1

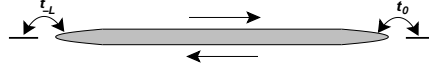


Fig. 2

Fig. 1 – Two Cooper pair boxes capacitively coupled to a quantum transmission line (equivalent circuit). The electric charge stored in the dashed box is conserved.

Fig. 2 – Two resonant levels coupled by tunnel junctions to the ends of a quantum wire of length  $L$ .

coupling constants

$$\beta_j = \frac{2C_j}{C_j + C_j^J + C_j^G} \sqrt{\frac{\mathcal{R}}{\hbar/e^2}}. \quad (3)$$

This Hamiltonian is a generalization of the Maxwell-Bloch Hamiltonian which has been used for modelling the interaction of two-level atoms with radiation [4]. Using the polaronic transformation,  $U = \prod_j \exp \{i\beta_j \Phi(j)(\sigma_j^z + 2n_j^G - 1)/2\}$ , (2) can be transformed into the double-Kondo Hamiltonian:

$$H_K = \frac{\hbar v}{2} \int_{-L}^0 (\hbar^{-2} \Pi^2 + (\partial_x \Phi)^2) dx - \frac{1}{2} \sum_j B_j^z \sigma_j^z - \frac{1}{2} \sum_j E_j^J (e^{i\beta_j \Phi(j)} \sigma_j^+ + \text{h.c.}) \quad (4)$$

Here  $B_j^z = 4E_j^c(1 - 2n_j^G)$  where  $E_j^c = e^2/2(C_j^J + C_j^G + C_j)$  is the charging energy of the qubit  $j$ . This model should not be confused with the two impurity Kondo model where the two magnetic impurities are in an infinite environment [9].

In the present physical situation, the total charge stored in the transmission line and the coupling capacitances is zero (see fig. 1). Assuming for simplicity  $\beta_0 = \beta_{-L} = \beta$ , this fixed charge constraint reads in the Kondo formulation:

$$\frac{1}{\beta} \int_{-L}^0 \hbar^{-1} \Pi(x) dx - \frac{1}{2} (\sigma_0^z + \sigma_{-L}^z) = n_0^G + n_{-L}^G - 1. \quad (5)$$

Using bosonization and taking care of Klein factors, the double-Kondo Hamiltonian with the same constraint can be shown to describe the low-energy physics of a 1D quantum wire of length  $L$  with resonant levels at its ends (see fig. 2). The effective low-energy theory of an isolated finite length Luttinger liquid [10] is characterized by a renormalized Fermi velocity  $v$  and a dimensionless interaction parameter  $g$  ( $g = 1$  for the Fermi liquid). This interaction parameter is related to  $\beta$  by  $\beta^2 = \pi/g$ . The Josephson energies are then proportional to the tunneling amplitudes between the wire and the resonant levels:  $E_j^J \propto t_j/\sqrt{a}$  where  $a$  is a microscopic length scale (UV cutoff). The magnetic fields  $B_j^z$  are related to the resonant level chemical potentials. The fixed charge condition (5) is obtained by working in the canonical ensemble: the total number  $\mathcal{N}$  of electrons in the wire plus the resonant levels is fixed. In this case, the r.h.s. of (5) is equal to  $\mathcal{N} + \chi - 1$  where  $e^{2i\pi\chi} = -e^{i(\theta_{-L} - \theta_0)}$  and  $\theta_j$  denotes the phase relating right to left moving fermions at the wire's ends:  $\psi_R(j) = e^{i\theta_j} \psi_L(j)$ .

The one-channel single impurity Kondo model consisting in a spin 1/2 coupled to a free boson on the half line has been shown to be integrable [11, 12]. Following [15] we conjecture that the double-Kondo problem is integrable for  $\beta_0 = \beta_{-L}$ . This opens the door to a general study of the thermodynamical properties of the double-Kondo model using integrable field

theory techniques [13,14] as done for the double sine-Gordon theory [16]. Such a study would go beyond the scope of the present letter and we shall therefore restrict ourselves to the Toulouse point where the problem can be treated in terms of fermions.

Fermionization of (4) is achieved by unfolding the free non-chiral boson onto a chiral boson  $\phi_R(x)$  living on an interval of length  $2L$  and, for  $\beta^2 = \pi$ , introducing the free chiral fermion  $e^{2i\beta\phi_R}$  on  $[-L, L]$ . Then, taking  $d_{-L} = \sigma_{-L}^+$ ,  $d_0 = (-1)^{n_{-L}}\sigma_0^+$  and  $\psi_R(x) = (-1)^{n_0+n_{-L}}(2\pi a)^{-1/2}e^{i\sqrt{4\pi}\phi_R(x)}$  ( $n_j = (1 - \sigma_j^z)/2$ ) defines a Jordan Wigner transformation which turns the boundary spins into fermionic degrees of freedom anti-commuting with the chiral fermion  $\psi_R$ . Because of the fixed charge condition, the fermionic field picks up a phase between  $-L$  and  $L$  which depends on the gate voltages:  $\psi_R(x + 2L) = -e^{2\pi i\chi}\psi_R(x)$  where  $\chi \equiv n_0^G + n_{-L}^G + 1/2 \pmod{1}$ . The fermionized form of (4) is then:

$$H_F = \int_{-L}^L \psi_R^\dagger(x)(-i\hbar v\partial_x)\psi_R(x) dx - \frac{1}{2} \sum_{j=-L,0} B_j^z(1 - 2d_j^\dagger d_j) + \sum_j H_j^\partial. \quad (6)$$

Boundary interactions  $H_j^\partial$  are given by:

$$H_{-L}^\partial = -\sqrt{\frac{\pi a}{2}} E_{-L}^J e^{i\pi\mathcal{N}} \left( e^{-i\pi(\chi-1/2)} d_{-L}^\dagger \psi_R(-L) + h.c. \right) \quad (7)$$

$$H_0^\partial = -\sqrt{\frac{\pi a}{2}} E_0^J \left( d_0^\dagger \psi_R(0) + h.c. \right) \quad (8)$$

where  $\mathcal{N}$  denotes the total number of fermions in the system. Because of the  $(-1)^\mathcal{N}$  operator in  $H_{-L}^\partial$ , we are not yet dealing with free fermions. The fixed charge constraint (5) simply means that the total number of fermions is fixed as well as the phase  $\chi$ . Therefore  $(-1)^\mathcal{N}$  is a phase that can be absorbed in a redefinition of  $d_{-L}$ . But as we shall see, (5) leads to unexpected subtleties in the computation of the thermodynamical properties of the system as functions of the physical parameters of the original qubit problem.

Since we are now dealing with free fermions, the ground state energy can be computed by summing one-particle energies up to the appropriate Fermi level. These are determined by the stationary wave condition:

$$1 + e^{2i(kL-\pi\chi)} R_0(k)R_{-L}(k) = 0 \quad (9)$$

where  $R_j(k) = (k - k_j - i\xi_j^{-1})/(k - k_j + i\xi_j^{-1})$  denotes the reflection matrix at boundary  $j$ . It can be expressed in terms of the boundary parameters  $\xi_j = 4\hbar^2 v^2 / \pi a (E_j^J)^2$  and  $k_j = B_j^z / \hbar v$ . As seen from  $R_j(k)$  expression, each qubit influences the modes of the line around  $k_j$  on a momentum scale  $\xi_j^{-1}$ . Up to a numerical factor,  $\hbar v / \xi_j$  is the energy scale associated with the Kondo boundary interaction<sup>(1)</sup> ( $\hbar\omega_B$  in [5]). At zero temperature, the finite frequency conductance of a Luttinger liquid with an impurity as well as the spectral function in dissipative quantum mechanics are functions of the variable  $\omega/\omega_B$  [17]. Moreover, the envelope of Friedel oscillations in a Luttinger liquid at  $g = 1/2$  is a function of the variable  $\omega_B x / v_F$  [18]. In this sense,  $\xi_j$  may be viewed as the Kondo length associated with each qubit.

We used the technique developed by Chatterjee for the 2D Ising model [19] to obtain an integral representation for the free energy of the system and therefore for its ground state energy. The final result is:

$$E_0 = \frac{\hbar v}{\pi} \int_{-\infty}^0 \left( L + \frac{\xi_j}{\xi_j^2(k - k_j)^2 + 1} \right) k dk - \frac{\hbar v}{2\pi} \int_0^{+\infty} \log(|1 + X(ik)|^2) dk. \quad (10)$$

---

<sup>(1)</sup>The parameter  $g$  in [5] corresponds to  $\beta^2/2\pi$  in the present letter. The Toulouse point in [5] is at  $g = 1/2$ .

where  $X(k) = e^{2i(kL - \pi\chi)} R_0(k) R_{-L}(k)$ . The first term, proportional to  $L$  is an extensive bulk contribution which does not depend on the qubit parameters. The second one is a boundary contribution which involves one boundary at a time. It will therefore not contribute directly to the correlations between the two qubits. Nevertheless, it contributes to the average population giving back the expected contribution for a resonant level connected to a semi-infinite Fermi liquid [20]. Correlations between the qubits are contained in the third term.

Equation (10) should however be taken with care. It corresponds to the energy of a ground state where only negative eigenstates are filled. But then, each time a one-particle energy level crosses zero, eq. (10) undergoes a discontinuity of its first derivative. On the other hand, the fixed charge constraint (5) tells us that the physical ground state of the system corresponds to a Dirac sea filled up to a Fermi level that varies with the physical parameters of the problem without crossing any one-particle energy levels. The physical ground state energy that incorporates the fixed charge condition should indeed be an analytical function of the qubit parameters. This is very similar to the analytical continuation introduced in [15] for the double sine-Gordon theory. Using the same method as for the ground state energy (10) integral representations for the populations and correlation of the qubits can be obtained and evaluated numerically, taking into account the fixed charge condition. Results depicted on figures 3 and 4 are obtained by this procedure.

Let us now discuss the results on correlations between the qubits induced by the transmission line. They are expected to depend on the ratios of  $\xi_{-L,0}/L$ . Naively, strong correlations may be expected when at least one of these lengths becomes comparable or larger than  $L$ , meaning that both qubits belong to the same large Kondo cloud. But indeed, only states whose wave vectors  $k$  satisfy  $|k - k_j| \xi_j \lesssim 1$  are significantly localized on the site associated with qubit  $j$ . Therefore strong correlations only occur when both Kondo lengths are comparable to  $L$ . For the same reason, it is also necessary that the two qubits influence the same modes of the line. This criterion should be seen as a variant of the exhaustion principle introduced by Nozières. Finally, strong correlations occur when both  $\xi_j$  are much larger than  $L$  and near degeneracy points  $B_0^z \sim B_{-L}^z$ .

For  $\xi_0 \gg L$  and  $\xi_{-L} \gg L$  the stationary wave condition (9) has two solutions that tend to  $k_0$  and  $k_{-L}$  with vanishing Josephson energies. Correlations appear when one of these special one-particle states is filled. Fig. 3 displays the average population of the  $x = 0$  qubit and the inter-qubit correlation  $C = \langle n_0 \rangle \langle n_{-L} \rangle - \langle n_0 n_{-L} \rangle$  as a function of the difference  $k_0 - k_{-L}$  and of  $\langle \mathcal{N} \rangle + \chi$  in the regime  $\xi_0 = \xi_{-L} \gg L$ . Fig. 4 shows the inter-qubit correlation in terms of the same variables but for different Kondo lengths illustrating the influence of asymmetry ( $\xi_0 \neq \xi_{-L}$ ):  $C$  still reaches its maximal value  $1/4$  but in a narrower zone. The two one-particle states close to  $k_{0,-L}$  give rise to an effective two-level system for the two lowest energy states of the system. Its effective Hamiltonian can be computed for  $\beta^2 < 2\pi$  using perturbation theory on the double-Kondo Hamiltonian<sup>(2)</sup>. This approach is valid as long as  $LE_j^J/\hbar v \ll \beta^2(L/\pi a)^{\beta^2/2\pi}$ . At degeneracy  $B_0^z = B_{-L}^z = B^z$  and for  $0 < u < 1$ , where  $u = 3/2 - (n_0^G + n_{-L}^G) + B^z L/\beta^2$ , the effective Hamiltonian in the space generated by  $|\uparrow\downarrow\rangle \otimes |\beta(n_0^G + n_{-L}^G - 1), \{0\}\rangle$  and  $|\downarrow\uparrow\rangle \otimes |\beta(n_0^G + n_{-L}^G - 1), \{0\}\rangle$  is of the form  $\Delta(X\sigma^z + \sigma^x)$  where

$$\Delta = \left(\frac{\pi a}{L}\right)^{\frac{\beta^2}{\pi}} \frac{E_{-L}^J E_0^J}{4\pi\hbar v/L} \frac{\Gamma(\frac{\beta^2}{\pi}u)\Gamma(\frac{\beta^2}{\pi}(1-u))}{\Gamma(\frac{\beta^2}{\pi})} \text{ and } X = \left( \left| \frac{E_0^J}{E_{-L}^J} \right| - \left| \frac{E_{-L}^J}{E_0^J} \right| \right) \frac{\sin(\beta^2(u - 1/2))}{2 \sin(\beta^2/2)}. \quad (11)$$

The correlation is then equal to  $C = 1/4(1 + X^2)$  and the energy separation between the

---

<sup>(2)</sup>IR divergences being cut by the finite size of the system, only UV divergences should be taken care of.

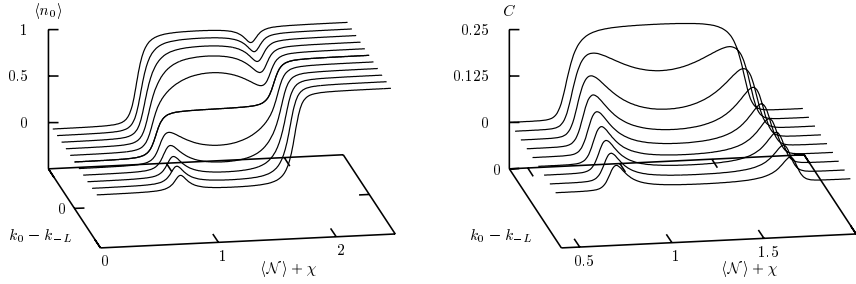


Fig. 3 – Average population  $\langle n_0 \rangle$  and correlation  $C = \langle n_0 \rangle \langle n_{-L} \rangle - \langle n_0 \cdot n_{-L} \rangle$  in the symmetric case  $E_0^J = E_{-L}^J$  such that  $\xi_0 = \xi_{-L} = 200 L$ . For the correlation, only the part with  $k_0 \geq k_{-L}$  has been represented since, in this case,  $C$  is an even function of  $k_0 - k_{-L}$ .

ground state and the first excited state is given by  $2\Delta\sqrt{1+X^2}$ . For  $E_0^J = E_{-L}^J$ , the two-qubit entanglement is maximal and the ground state is given by  $\frac{1}{\sqrt{2}}(|\uparrow\downarrow\rangle + |\downarrow\uparrow\rangle) \otimes |\beta(n_0^G + n_{-L}^G - 1), \{0\}\rangle$ . Note that nevertheless entanglement is lost when going back to the original qubit problem because of the orthogonality effect induced by the polaronic transformation: qubit states  $|\downarrow\uparrow\rangle$  and  $|\uparrow\downarrow\rangle$  get correlated to different states of the transmission line whose scalar product goes as  $(a/L)^{\beta^2/\pi}$ . As expected, entanglement can appear in the original qubit problem for small  $\beta^2$ : for  $E_j^c, E_j^J \ll \hbar v/L$  integration over the modes of the line gives an effective static coupling of the form  $(v\beta^2/4L)\sigma_0^z\sigma_{-L}^z$ . This is the regime usually considered for quantum computation.

When one of the  $\xi_j$  is much smaller than  $L$ , the corresponding qubit renormalizes onto a conformally invariant boundary condition. This regime is reached in the limit of very large Josephson energy and corresponds to the strong coupling limit of the Kondo problem. The corresponding quantum impurity is totally screened and therefore is not seen by the other one. Then, when either  $\xi_0 \ll L$  or  $\xi_{-L} \ll L$ , the correlation  $C$  is expected to vanish (Kondo regime). This is confirmed by our exact results but we can also study the crossover where one of the  $\xi_j$  is much larger than  $L$  and the other varies. For  $L \ll \xi_{-L}$  and  $\xi_0 \sim L$ , our analysis for  $\beta^2 = \pi$  predicts a maximum absolute value of correlation between the qubits decaying as  $1/4(1 + L/\xi_0)$ . Fig. 5 displays the maximal  $C$  as a function of  $L/\xi_0$  and  $L/\xi_{-L}$ .

To summarize, we have described a common approach to the problem of two qubits coupled via a finite length quantum transmission line and to the problem of two resonant levels at the ends of a finite length quantum wire. These two problems can be mapped to the double-Kondo model with a fixed charge constraint. At its Toulouse point, we have solved the model exactly enabling an explicit analysis of the correlation between the quantum impurities (qubits or resonant levels) through their common environment. The emergence of correlations is related to the overlap of the influence zones (Kondo clouds) of each quantum impurity in reciprocal space. We stress that the same techniques can be extended to obtain results on dynamical correlation functions. This gives a direct access to the absorption spectrum of the system when excited by a microwave radiation sent on one of the available gates. The correlations between the charge of each qubit and the charge density along the line can also be obtained exactly as well as the Friedel oscillations induced by the resonant levels at the ends in the quantum wire problem. These correlations provide a direct insight into the Kondo cloud in real space.

Based on our study at the Toulouse point and on the perturbative approach at  $\beta^2 < 2\pi$ , our conclusions on the role of Kondo lengths on inter-qubit correlations should hold for  $\beta^2 < 2\pi$ .

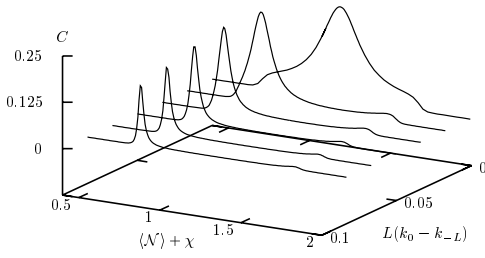


Fig. 4

Fig. 4 – The correlation  $C$  for  $\xi_{-L}/\xi_0 = 20$ ,  $\xi_0/L = 200$ .

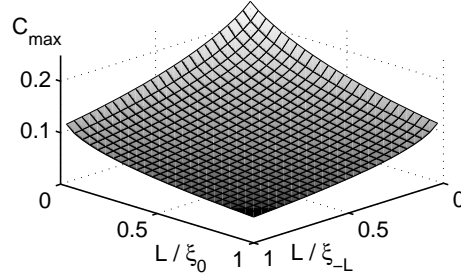


Fig. 5

Fig. 5 – The maximum of  $C$  in the  $(k_0 - k_{-L}, \mathcal{N} + \chi)$  plane as a function of  $L/\xi_0$  and  $L/\xi_{-L}$ .

This remains to be fully confirmed by analytical computations in the non perturbative regime away from  $\beta^2 = \pi$ . From an experimental point of view, the quantum wire design is suitable for exploring the region around the Toulouse point. Since transmission line impedances are in the current status of technology bounded by a few hundred Ohms, the qubit design is unfortunately limited to  $\beta \lesssim 0.3$  but both schemes provide complementary ways to explore the same physics.

\* \* \*

P. Degiovanni would like to acknowledge Boston University for hospitality while this work was completed and C. Chamon for a careful reading of the manuscript.

## REFERENCES

- [1] BRUNE M., RAIMOND J.-M. and HAROCHE, S., *Rev. Mod. Phys.*, **73** (2001) 565
- [2] MAKHLIN YU., SCHÖN G. and SHNIRMAN, A., *Rev. Mod. Phys.*, **73** (2001) 357
- [3] BLAIS A., HUANG R.-S., WALLRAFF A., GIRVIN S. M. and SCHOELKOPF, R. J., *Phys. Rev. A*, **69** (2004) 062320
- [4] LECLAIR A., *Ann. Phys.*, **271** (1999) 268
- [5] LECLAIR A., LESAGE F., LUKYANOV S. and SALEUR, H., *Phys. Lett. A*, **235** (1997) 203
- [6] CEDRASCHI P. and BÜTTIKER M., *Ann. of Phys.*, **289** (2001) 1
- [7] AFFLECK I. and SIMON, P., *Phys. Rev. Lett.*, **86** (2001) 2854
- [8] BARDAKCI K. and KONECHNY A., *Nucl. Phys. B.*, **598** (2001) 427
- [9] JAYAPRAKASH P., KRISHNA-MURTHY H.R. and WILKINS J.W., *Phys. Rev. Lett.*, **47** (1981) 737
- [10] FABRIZIO M. and GOGOLIN A. O., *Phys. Rev. B*, **51** (1995) 17827
- [11] ANDREI N., FURUYA K. and LOWENSTEIN, J.H., *Rev. Mod. Phys.*, **55** (1983) 331
- [12] TSVELICK, A.M. and WIEGMAN, P.B., *Adv. Phys.*, **32** (1983) 453
- [13] GHOSHAL S. and ZAMOLODCHIKOV A., *Int. J. of Mod. Phys. A*, **9** (1994) 3841
- [14] FENDLEY P., *Phys. Rev. Lett.*, **71** (1993) 2485
- [15] CAUX J.-S., SALEUR, H. and SIANO, F., *Phys. Rev. Lett.*, **88** (2002) 106402
- [16] CAUX J.-S., SALEUR H. and SIANO, F., *Nucl. Phys. B*, **672** (2003) 411
- [17] LESAGE F., SALEUR H. and SKORIC, S., *Nucl. Phys. B*, **474** (1996) 602
- [18] LECLAIR A., LESAGE F. and SALEUR H., *Phys. Rev. B*, **54** (1996) 13597
- [19] CHATTERJEE R., *Mod. Phys. Lett. A*, **10** (1995) 973
- [20] FURUSAKI A. and MATVEEV K. A., *Phys. Rev. Lett.*, **88** (2002) 226404